Cancer Cell
Article

Deletion of *p120-Catenin* Results in a Tumor Microenvironment with Inflammation and Cancer that Establishes It as a Tumor Suppressor Gene

Douglas B. Stairs,[1,2,4,5] Lauren J. Bayne,[8] Ben Rhoades,[1,5] Maria E. Vega,[1,5] Todd J. Waldron,[1,5] Jiri Kalabis,[1,5] Andres Klein-Szanto,[6] Ju-Seog Lee,[7] Jonathan P. Katz,[1,5] J. Alan Diehl,[5,8] Albert B. Reynolds,[9] Robert H. Vonderheide,[2,5,8] and Anil K. Rustgi[1,2,3,5,*]

[1]Division of Gastroenterology
[2]Department of Medicine
[3]Department of Genetics
University of Pennsylvania, Philadelphia, PA 19104, USA
[4]Department of Pathology and Laboratory Medicine, Penn State College of Medicine, Hershey, PA 17033, USA
[5]Abramson Cancer Center, University of Pennsylvania, Philadelphia, PA 19104-3309, USA
[6]Histopathology Facility, Fox Chase Cancer Center, Philadelphia, PA 19111-2497, USA
[7]Department of Systems Biology, MD Anderson Cancer Center, Houston, TX 77030, USA
[8]Department of Cancer Biology and Abramson Family Cancer Research Institute, University of Pennsylvania, Philadelphia, PA 19104-3309, USA
[9]Department of Cancer Biology, Vanderbilt University, Nashville, TN 37232-6840, USA
*Correspondence: anil2@mail.med.upenn.edu
DOI 10.1016/j.ccr.2011.02.007

SUMMARY

p120-catenin (p120ctn) interacts with E-cadherin, but to our knowledge, no formal proof that p120ctn functions as a bona fide tumor suppressor gene has emerged to date. We report herein that p120ctn loss leads to tumor development in mice. We have generated a conditional knockout model of *p120ctn* whereby mice develop preneoplastic and neoplastic lesions in the oral cavity, esophagus, and squamous forestomach. Tumor-derived cells secrete granulocyte macrophage colony-stimulating factor (GM-CSF), macrophage colony-stimulating factor (M-CSF), monocyte chemotactic protein-1 (MCP-1), and tumor necrosis factor-α (TNFα). The tumors contain significant desmoplasia and immune cell infiltration. Immature myeloid cells comprise a significant percentage of the immune cells present and likely participate in fostering a favorable tumor microenvironment, including the activation of fibroblasts.

INTRODUCTION

Cell-cell junctions are critical for cell adhesion during normal epithelial homeostasis. The cardinal feature of the adherens junctions is the interaction between the cytoplasmic tail of classical type I (E-cadherin) and type II cadherins, and p120-catenin (p120ctn, also referred to as catenin, delta1, or Ctnnd1), which engenders stability of this specific junctions complex at the cell membrane (Davis et al., 2003; Ireton et al., 2002; Xiao et al., 2003). Recently, it was revealed by X-ray crystallography that p120 isoform 4A is in complex with the juxtamembrane domain core region (JMD(core)) of E-cadherin (Ishiyama et al., 2010). Loss of p120ctn or its phosphorylation on serine-threonine residues is able to destabilize E-cadherin (Fukumoto et al., 2008). Thus, p120ctn regulates cadherin stability and turnover. The balance between adhesion and migration is regulated further by p120ctn's ability to regulate the activities of RhoA, Rac, and Cdc42 through the amino terminus of p120ctn, thereby orchestrating exquisite actin dynamics (Reynolds and Roczniak-Ferguson, 2004). Furthermore, the bridge between p120ctn and

Significance

Oral squamous cell cancers (OSCCs) and esophageal squamous cell cancers (ESCCs) represent common human cancers worldwide. The molecular pathogenesis underlying these cancers involves p120-catenin (p120ctn), which is critical to epithelial homeostasis through the adherens junctions. p120ctn loss or mislocalization in these specific cancers served as a basis for the generation of a conditional knockout mouse model, revealing a dramatic invasive squamous cell cancer phenotype accompanied by induction of prosurvival signals, desmoplasia, and recruitment of immature myeloid cells. Thus, p120ctn loss in this mouse model proves its tumor suppressor role and establishes a platform for strategies designed for early detection, molecular imaging, and targeted therapeutics in these cancers that have been elusive to date.

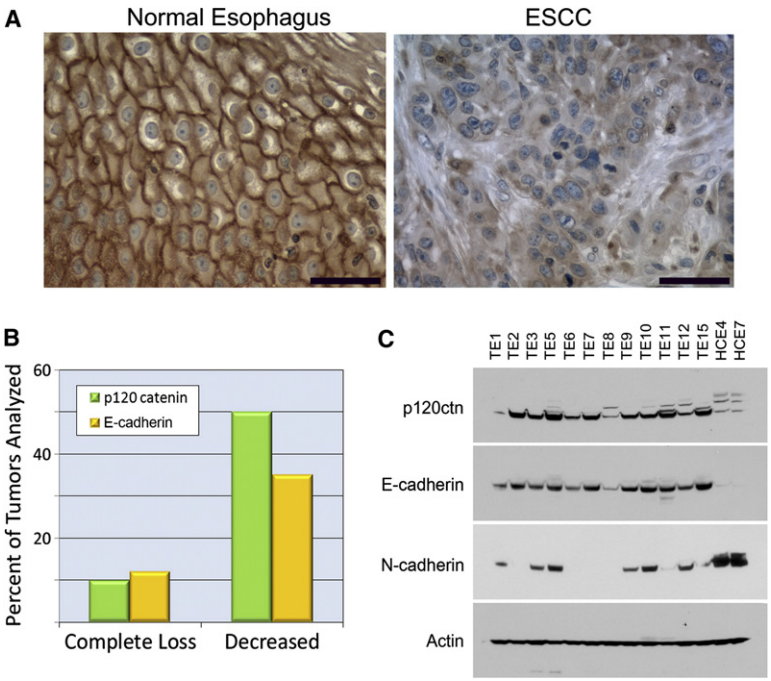

Figure 1. p120ctn and E-Cadherin Expression in ESCC

(A) p120ctn expression by IHC reveals cell membrane localization in normal tissue, whereas cytoplasmic mislocalization and decreased or absent expression are detected in ESCC. Scale bars, 50 μM.

(B) Quantification of p120ctn and E-cadherin expression in ESCC relative to matched adjacent normal esophagus (n = 69 paired samples). Fisher's exact analysis demonstrates that p120ctn and E-cadherin expression is coordinately regulated ($p = 0.017$).

(C) Western blot analysis of human esophageal cancer cell lines for p120ctn, E-cadherin, and N-cadherin expression, with β-actin as loading control.

these effectors of migration involves p190RhoGAP (Wildenberg et al., 2006).

p120ctn's structure is highlighted by an amino-terminal domain that has regulatory functions, a central Armadillo Repeat domain (Arm), a nuclear export signal (NES), and a carboxyl-terminal domain whose function(s) remains to be elucidated (Anastasiadis et al., 2000). Isoforms of p120ctn result from differential splicing. Initiation at the first ATG start site (Isoform 1) results in preferential expression in the mesenchymal compartment, whereas isoforms that lack a coiled-coiled domain that utilize the third start site (Isoform 3) are expressed in the epithelial compartment. Not all isoforms express the NES.

It has become increasingly clear that loss, downregulation, or mislocalization of p120ctn helps to define diverse tumor types in the prostate, breast, pancreas, colon, skin, bladder, and endometrium (Reynolds and Roczniak-Ferguson, 2004; Thoreson and Reynolds, 2002; van Hengel and van Roy, 2007). Interestingly, decreased expression is not typically observed in the entire tumor but rather in regions of the tumor, similar to that observed for E-cadherin loss (Birchmeier, 1995). This loss or mislocalization of p120ctn frequently leads to E-cadherin destabilization, endowing a cancer cell an advantage in cell migration by virtue of abrogation of cell adhesion. Additionally, knockdown experiments using shRNA to p120ctn have demonstrated that p120ctn loss induces invasion in tumor cell lines with concomitant loss or downregulation of E-cadherin (Macpherson et al., 2007), although collective invasion might involve also concurrent retention of membranous p120ctn and cadherin-mediated (P- or E-cadherin) cell-cell contacts at least in vitro. In aggregate, these data suggest a potential tumor suppressor role for p120ctn in various cancer types, but to our knowledge, a causal role in vivo has yet to be demonstrated unequivocally.

p120ctn loss in the mouse has been modeled in an attempt to phenocopy human disease, but to date, no published mouse model has yielded a cancer phenotype. Deletion of *p120ctn* by homologous recombination in mice results in embryonic lethality. Tissue-specific targeting of *p120ctn* has been utilized to study the role of *p120ctn* in development and tumorigenesis (Davis and Reynolds, 2006). For example, p120ctn loss results in impaired enamel development (Bartlett et al., 2010). Targeted *p120ctn* deletion in the embryonic salivary gland forces a loss of acinar development and an adoption of a ductal cell fate. Although these mice die immediately in the postnatal period, the salivary glands are distinguished by intraepithelial dysplasia, but not cancer (Davis and Reynolds, 2006). p120ctn loss in the skin results in epidermal hyperplasia and chronic inflammation with loss of hair and body fat (Perez-Moreno et al., 2006). Furthermore, the epidermis has evidence of NFκB activation and mitotic defects such as aneuploidy, but no overt cancer (Perez-Moreno et al., 2008). Recently, conditional p120ctn loss in the small intestine and colon was found to result in death by 21 days, with evidence of mucosal erosion and bleeding, and recruitment of COX-2 expressing neutrophils, suggesting an underlying barrier defect (Smalley-Freed et al., 2010). Thus, to date, and to our knowledge, no tissue-specific p120ctn knockout mouse models have been able to demonstrate that p120ctn loss results in the development of invasive cancer.

The overarching goal of this study was to generate and characterize mechanistically a genetic mouse model in which conditional p120ctn loss in the squamous oral cavity, esophagus, and forestomach results in cancer that phenocopies precisely the histologic features of human oral and esophageal squamous cell carcinomas (OSCCs, ESCCs, respectively). In so doing, such a model might provide a platform for the consideration of combinatorial therapeutics in ESCCs, OSCCs, and potentially other squamous cell cancers.

RESULTS

p120ctn Expression Is Lost or Reduced in Esophageal Cancer Tissues and Cell Lines

A human tissue microarray (TMA) with matched normal esophageal and esophageal squamous cell cancer (ESCC) tissues was evaluated for p120ctn expression by immunohistochemistry (IHC) (Figure 1A). p120ctn has the expected membrane-associated localization in the normal esophageal squamous epithelium.

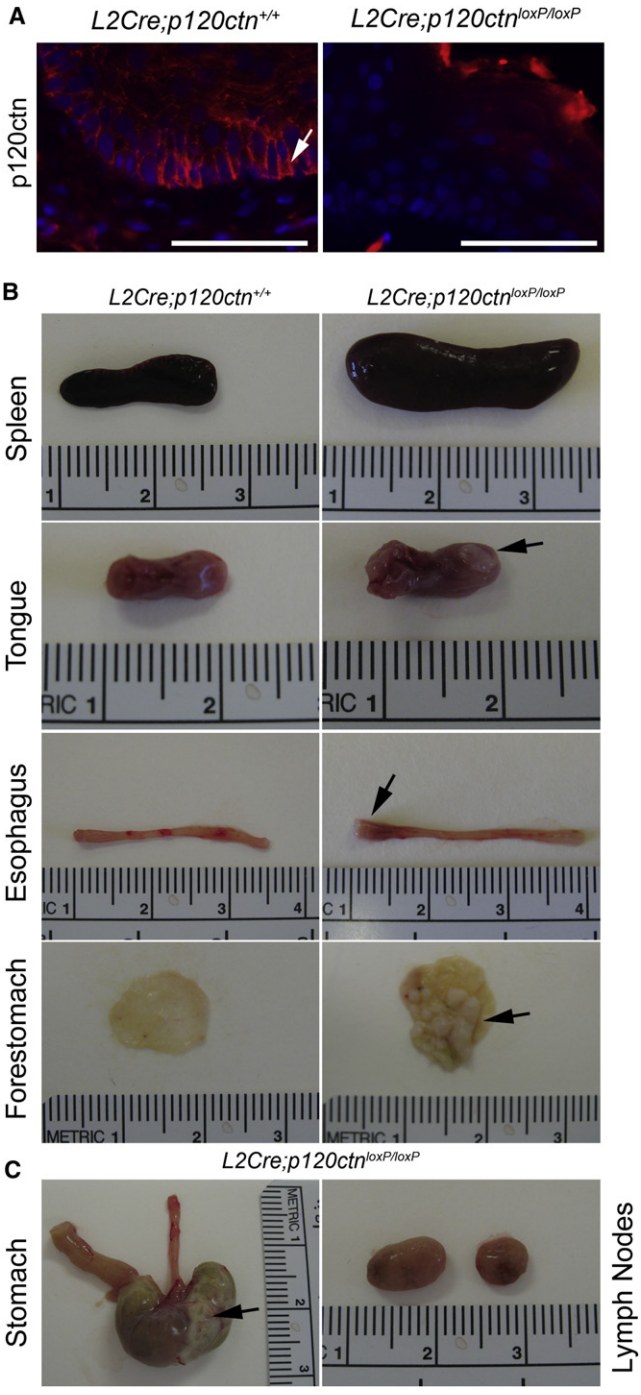

Figure 2. Gross Pathology of *L2Cre;p120ctn*$^{loxP/loxP}$ Mice

(A) Two-month-old mice were analyzed by IF for p120ctn expression. Arrow indicates normal cell membrane localization in *L2Cre;p120ctn*$^{+/+}$ esophagi (n = 4). p120ctn loss is evident in the esophagi of *L2Cre;p120ctn*$^{loxP/loxP}$ mice (n = 4). Nonspecific staining of keratins can be observed in the cornified layers. Scale bars, 50 μM.

(B) Gross lesions were detected in the spleen, tongue, esophagus, and squamous forestomach of 9- to 12-month-old *L2Cre;p120ctn*$^{loxP/loxP}$ mice. A reference ruler (centimeters) is included in each image for size comparison. Arrows indicate the location of tumors.

(C) Gross pathology of a squamous forestomach tumor (indicated by an arrow) and two enlarged lymph nodes (normally approximately 1–2 mm in diameter) from a *L2Cre;p120ctn*$^{loxP/loxP}$ mouse. See also Table S1 and Figure S1. A total of 23 *L2Cre;p120ctn*$^{loxP/loxP}$ mice and 23 control (five p120ctn$^{loxP/loxP}$, ten *L2Cre;p120ctn*$^{+/+}$, and eight *L2Cre;p120ctn*$^{+/loxP}$) mice were evaluated.

By contrast, 100% of the 69 ESCC tumors have p120ctn loss or cytoplasmic mislocalization (Figure 1B). There is a statistically significant association ($p = 0.017$) between decreased p120ctn and E-cadherin expression with odds ratio = 3.23 (95% CI: $1.13 < O.R. < 9.24$). These data reveal that p120ctn and E-cadherin are coordinately decreased or lost in the majority of ESCCs, and substantiate previous findings (Chung et al., 2007).

A panel of 14 human esophageal squamous tumor cell lines was analyzed for p120ctn and E-cadherin expression (Figure 1C). p120ctn expression was detected in all cell lines with different isoforms observed in a subset of them. E-cadherin expression was moderate to high in 11 of 14 cell lines, low in one (TE8), and absent in two cell lines (HCE4, HCE7). p120ctn and E-cadherin expression correlated well in the cell lines. Interestingly, the mesenchymal p120ctn isoform appears to be expressed in HCE-4 and HCE-7 cells along with N-cadherin, consistent with N-cadherin's pattern of known mesenchymal expression.

Conditional Deletion of *p120ctn* in the Oral Cavity, Esophagus, and Forestomach Results in Invasive Squamous Cell Cancer, Desmoplasia, and Inflammation

To elucidate the mechanistic roles of p120ctn in vivo, we generated spatially targeted p120ctn deletion in the squamous oral cavity, esophagus, and forestomach. We bred *L2Cre* and *p120*$^{loxP/loxP}$ mice together to generate *L2Cre;p120*$^{loxP/loxP}$ mice, where the *L2* promoter is active specifically in the squamous oral cavity, esophagus, and forestomach (Nakagawa et al., 1997; Opitz et al., 2002). *LacZ* (*Gt(Rosa) 26*^{Tm1Sor}) reporter mice were crossed with *L2Cre* mice to determine the efficiency of *Cre* recombination in the oral cavity, esophagus, and forestomach of mice. LacZ staining demonstrates effective recombination and, therefore, Cre expression in these specific tissues (see Figure S1 available online). To verify p120ctn loss in *L2-Cre;p120*$^{loxP/loxP}$ mice, p120ctn protein expression was assessed by immunofluorescence (IF). p120ctn was effectively lost in the epithelium in 2-month-old *L2-Cre;p120*$^{loxP/loxP}$ mice compared to *L2-Cre;p120*$^{+/+}$ control mice (Figure 2A).

Gross pathology examination of the oral cavities, esophagi, and forestomachs of *L2Cre;p120*$^{loxP/loxP}$ mice revealed significant masses in each of these tissues, along with splenomegaly and local lymphadenopathy (Figures 2B and 2C). Histologic analysis at 4–6 months of age revealed epithelial dysplasia (data not shown). Histologic analysis at 9–12 months of age demonstrated severe dysplasia with invasive squamous cancer into the submucosa and muscle in *L2Cre;p120*$^{loxP/loxP}$ mice, whereas all control mice (*p120*$^{flox/flox}$, *L2-Cre;p120*$^{+/+}$, and *L2-Cre;p120*$^{+/loxP}$) had no abnormalities (Figure 3A). Approximately 70% of *L2Cre;p120*$^{loxP/loxP}$ mice develop tumors between 9 and 12 months of age, whereas no tumors were detected in age-matched littermate control mice (Table S1; $p < 0.0001$). Invasive esophageal cancer was detected as early as 4 months of age in one *L2Cre;p120*$^{loxP/loxP}$ mouse. Some esophageal tumors were poorly differentiated but displayed no evidence of any obvious distant metastasis, although we cannot

exclude the possibility of micrometastasis in other organs (Figure 3A). The submucosa was altered with marked desmoplasia and the striking presence of immune cell infiltration (Figure 3A).

Analysis of *L2-Cre;p120*$^{loxP/loxP}$ forestomachs revealed severe hyperplasia, severe dysplasia, and invasive cancers into the underlying desmoplastic and inflammatory stroma. (Figure 3A). The forestomachs of all control mice (*p120*$^{flox/flox}$, *L2-Cre;p120*$^{+/+}$, and *L2-Cre;p120*$^{+/loxP}$) revealed no morphologic changes (Figure 3A). Nearly identical results are evident in the oral cavities of *L2-Cre;p120*$^{loxP/loxP}$ mice, namely invasive squamous cell cancer with desmoplasia and immune cell infiltration (Figure 3A).

We next evaluated E-cadherin expression in *L2-Cre;p120*$^{loxP/loxP}$ mice. Significant loss of E-cadherin expression is noted in *L2-Cre;p120*$^{loxP/loxP}$ mice compared to *L2-Cre;p120*$^{+/+}$ control mice, with residual E-cadherin expression in some *L2-Cre;p120*$^{loxP/loxP}$ mice where it is cytoplasmic (Figure 3B). In some mice, whereas p120ctn is lost and E-cadherin is either lost or cytoplasmic, there are occasional focal areas within tumors that retain both p120ctn and E-cadherin at the cell membrane (Figure 3C), the latter consistent with the notion of collective invasion observed in A431 cells in vitro (Macpherson et al., 2007).

Alterations in Proliferation and Differentiation in *L2-Cre/p120*$^{flox/flox}$ Mice

Ki-67 and keratin 14 (K14), markers of proliferation, were evaluated in esophageal tumors from *L2-Cre;p120*$^{loxP/loxP}$ mice. Normal proliferating basal cells express Ki-67 and K14, whereas normal differentiated suprabasal cells express keratins 4 and 13 (K4, K13, respectively) and harbor little proliferation. Ki-67 expression was significantly increased in the esophageal epithelia and in the invasive cancers in *L2-Cre;p120*$^{loxP/loxP}$ mice compared to control mice (Figure S2; $p = 3 \times 10^{-6}$). K14 expression was increased in the esophageal epithelia at 5 months of age, which ultimately expanded to the luminal surface by 12 months of age (data not shown). K4 expression, as evaluated by qPCR, is decreased 2.5-fold ($p = 0.014$) in *L2-Cre;p120*$^{loxP/loxP}$ mice compared to *L2-Cre;p120*$^{+/+}$ control mice (data not shown). Invading tumor cells are K14 positive (Figure 3C). Interestingly, β-catenin expression was membranous in the esophagi of *L2-Cre;p120*$^{loxP/loxP}$ mice (Figure 3C) but lost in the oral cavity of the *L2-Cre;p120*$^{loxP/loxP}$ mice. Furthermore, no alterations were apparent for epidermal growth factor receptor (EGFR), c-*myc*, or K-ras by IHC in the tumors (data not shown). However, p-Akt (but not p-Erk1/2 [p-Mapk]) was increased in the tumors, as was p-Stat3, which might contribute to tumorigenesis (Figure S2).

NFκB and Inflammatory Cells in the Tumor Microenvironment

Given the significant recruitment of immune cells in the tumor stroma, we hypothesized that NFκB activation may be present in these lesions, as has been reported previously (Perez-Moreno et al., 2006; Perez-Moreno et al., 2008). Indeed, this was confirmed with robust NFκB induction in dysplasia and tumors, thereby suggesting that this is an early event (Figure 4A). The NFκB induction was evident also in the immune cells found in the tumor stroma (Figure 4A).

We then established cells from an esophageal tumor (designated as 714ET) as well as esophageal cell lines from *p120ctn*$^{loxP/loxP}$ mice that in turn were infected with retroviral Cre recombinase or a control vector (designated as F2-Cre and F2-Tomato, respectively). Western blot analysis revealed complete p120ctn loss in both F2-Cre and 714ET cells and retained p120ctn expression in the control F2-Tomato cells (Figure 4B and quantified in Figure 4C, left panel). In F2-Cre and 714ET cells, there is activated p-NFκB (8-fold), p-Akt (4-fold), and p-Stat3 (2-fold) (Figures 4B and 4C). Additionally, 714ET cells were found to secrete significant amounts of granulocyte macrophage colony-stimulating factor (GM-CSF), macrophage colony-stimulating factor (M-CSF), monocyte chemotactic protein-1 (MCP-1), and tumor necrosis factor-α (TNFα) (Figure 4D), but not other cytokines tested (IL-1β, IL-2, IL-4, IL-5, IL-6, or IFNγ; data not shown). GM-CSF has been suggested to contribute to immature myeloid cell recruitment (Marigo et al., 2010).

In order to characterize the immune cells in the tumor microenvironment, we undertook a number of experiments. Splenic weights in *L2-Cre;p120*$^{loxP/loxP}$ mice were 5-fold greater than in control mice ($p = 0.0004$), and there was also leukocytosis with increased segmented neutrophils, band neutrophils, eosinophils, and monocytes (Table S2). These findings suggested that there may be an elevated production of circulating myeloid lineage cells and that the invasive squamous cell cancers in the *L2-Cre;p120*$^{loxP/loxP}$ mice might contribute to the recruitment of these immune cells. Therefore, we analyzed the leukocyte fraction (CD45+ cells) for immature myeloid cells (defined phenotypically as Gr-1+ CD11b+ cells), macrophages (F4/80+), T cells (CD3+), B cells (CD19+), dendritic cells (CD11c+), and natural killer (NK) cells (CD49b+). The percentage of CD45+ cells was approximately the same for normal versus dysplastic versus tumor tissues and spleens (Figure 4E). However, there was a statistically significant increase (Figure S3) in immature myeloid cell infiltration in dysplastic and tumor tissues (Figure 4E). In dysplastic esophagi or forestomachs, the percentage of immature myeloid cells increased 4- to 8-fold compared to control tissues (<5% of CD45+ cells) (Figure 4F). The percentage of immature myeloid cells was higher also in esophageal and forestomach tumors (Figure 4F). Other types of immune cells (macrophages, T cells, B cells, dendritic cells, NK cells) did not increase with dysplasia and cancer (Figures 4E; Figure S3).

The fact that only one subpopulation of immune cells (immature myeloid cells) is specifically increased suggests that p120ctn loss may lead to a highly selective process of immune cell recruitment. We next purified splenic Gr-1+ CD11b+ cells and prepared cytospins for cytology (Figure S3). Staining and quantification revealed that the Gr-1+ CD11b+ cells represent a range of cells, including myelocytes/metamyelocytes (11.7%), segmented neutrophils (48.1%), band neutrophils (12.5%), and monocytoid cells (7.7%). These cells have activated nuclear NFκB (Figure S3), consistent with what was found in the mouse tumors (Figure 4A).

In order to evaluate the functional properties of the immature myeloid cells, we again purified Gr-1+ CD11b+ cells from tumor-bearing *L2-Cre;p120*$^{loxP/loxP}$ mice and found that these cells inhibited peptide-specific T cell responses in vitro (using OVA-specific TCR-transgenic T cells) (Figure 4G).

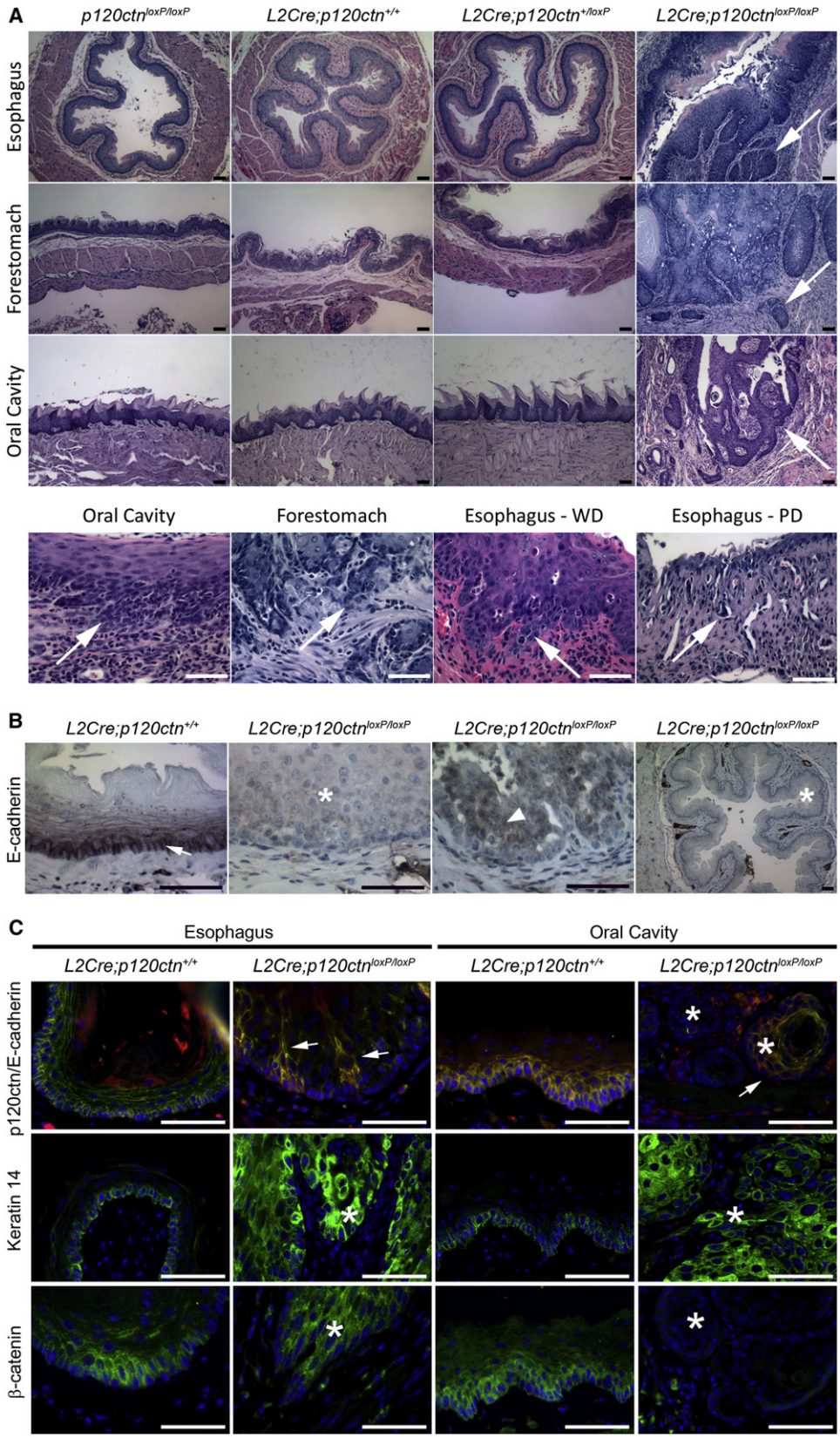
A
p120ctn loxP/loxP
L2Cre;p120ctn +/+
L2Cre;p120ctn +/loxP
L2Cre;p120ctn loxP/loxP
Esophagus
Forestomach
Oral Cavity
Oral Cavity
Forestomach
Esophagus - WD
Esophagus - PD
B
L2Cre;p120ctn +/+
L2Cre;p120ctn loxP/loxP
L2Cre;p120ctn loxP/loxP
L2Cre;p120ctn loxP/loxP
E-cadherin
C
Esophagus
Oral Cavity
L2Cre;p120ctn +/+
L2Cre;p120ctn loxP/loxP
L2Cre;p120ctn +/+
L2Cre;p120ctn loxP/loxP
p120ctn/E-cadherin
Keratin 14
β-catenin

Additionally, these immature myeloid cells produce nitric oxide and have been suggested to suppress T cells (Figure 4H) (Bronte et al., 2003; Bronte and Zanovello, 2005). We next treated *L2-Cre;p120*$^{loxP/loxP}$ mice with dexamethasone and found a dramatic attenuation of esophageal tumor invasion to that of hyperplasia (Figures 5A; Figure S4). CD45+ cells and Gr-1+CD11b+ cells were quantified by flow cytometry and were reduced (Figure 5B; data not shown). We analyzed further these Gr-1+CD11b+ cells and found decreased IL-4Rα expression in the dexamethasone-treated mice (Figure 5C). Notably, IL-4Rα expression on Gr-1+CD11b+ cells has been reported to correlate with suppression of CD8+ T cells (Gallina et al., 2006; Mandruzzato et al., 2009). These data suggest that inflammatory cells, including the Gr-1+CD11b+ cells, are fostering tumorigenicity.

Desmoplasia Is Present in the Tumor Microenvironment

To evaluate the specific features of the microenvironment in the invasive cancers that develop in *L2-Cre;p120*$^{loxP/loxP}$ mice, a pronounced increase in fibrillar collagen was present in the tumor stroma consistent with the desmoplasia in human ESCC and OSCC (Figure 5D). By contrast, fibrillar collagen is localized to a narrow region below the epithelium (Figure 5D). Additionally, there was increased fibroblast specific protein-1 (Fsp1) expression in mouse OSCC and ESCC (Figure 5E). Similarly, α-smooth muscle actin (αSMA) was increased in the mouse tumors (data not shown). Interestingly, dexamethasone-treated mice had resolution of the desmoplasia with little residual Fsp1+ fibroblasts (Figures 5E and 5F; Figure S4), suggesting a possible role for the immune system in regulating desmoplasia in our model system.

To evaluate a potential link between immature myeloid cell inflammation and desmoplasia, we next conducted coculture of purified Gr-1+CD11+ cells from tumor-bearing *L2-Cre;p120*$^{loxP/loxP}$ mice with normal fibroblasts (from C57BL/6 mice) and cancer (OSCC, ESCC) associated fibroblasts (CAFs) (from *L2-Cre;p120*$^{loxP/loxP}$ mice) that revealed activation of the normal fibroblasts and further augmentation of CAFs based upon αSMA and Fsp1 expression (Figures 6A–6C). In fact, some of the activated CAFs have an interesting ''dendritic'' appearance in coculture and display a similar morphology in mouse tumors (Figure 6C). Furthermore, the Gr-1+CD11+ cells survived better and expressed higher IL-4Rα levels in coculture with CAFs (Figure 6D).

Given the different lines of evidence for the tumor-promoting role of Gr-1+CD11+ cells in *L2-Cre;p120*$^{loxP/loxP}$ mice, we next sought to determine a relationship between myeloid cells and p120ctn loss in human ESCC. Increased myeloperoxidase (MPO) staining in the tumor stroma for myeloid lineage cells correlates with p120ctn loss (Figure 7A; $p = 0.05$). This raises the possibility that p120ctn loss might induce the recruitment of MPO+ cells in the pathogenesis of human ESCC.

Secondary Alterations in Invasive Squamous Cell Cancers

Apart from enhanced activation of NF-κB, Akt, and Stat-3 in the tumor cells, and the probability that GM-CSF, MCP-1, and TNFα are induced by NFκB in the tumor cells (Schreck and Baeuerle, 1990), we have begun to identify potential secondary alterations in p120ctn-deficient squamous epithelia that may contribute to cancer development. RNA microarray analysis was performed using isolated epithelia from the esophagi and forestomachs from 12-month-old *L2-Cre;p120*$^{loxP/loxP}$ mice and *L2-Cre/p120*$^{+/+}$ control mice. Unsupervised hierarchical clustering was performed and identified significantly altered genes (Figure S5). Several genes involved in cytokine signaling, *IL-13Ra1*, *IL-1R2*, and *Pias1*, are altered in p120-deficient squamous epithelia based upon microarray analysis and were confirmed by qPCR (Figure S5).

DISCUSSION

p120-ctn Loss Results in Invasive Squamous Cell Cancer

The complex between E-cadherin and p120-ctn is critical for the formation and maintenance of the adherens junctions. Disruption of this complex is a hallmark feature of epithelially derived cancers. p120ctn loss or mislocalization can destabilize E-cadherin. Definitive proof for p120ctn's functional role as a tumor suppressor gene in vivo has been elusive to date. Targeted disruption of murine *p120ctn* in the salivary gland (*MMTV-cre;p120ctn*$^{flox/flox}$), skin (*K14-cre;p120ctn*$^{flox/flox}$), and intestine (*Villin-Cre; p120ctn*$^{flox/flox}$) does not result in cancer (Davis and Reynolds, 2006; Perez-Moreno et al., 2006; Smalley-Freed et al., 2010). p120ctn may not be critical for tumor suppression in these specific tissues. Alternatively, a lack of tumor formation in these mice may be due to early death. Generation and characterization of *L2-Cre;p120*$^{loxP/loxP}$ mice result in a dramatic phenotype of invasive cancer in the oral cavity, esophagus, and forestomach. These cancers may be either unifocal or multifocal, and there is preceding severe dysplasia, underscoring a temporal progression from preneoplasia to neoplasia, mirroring human OSCC and ESCC progression.

How does p120ctn loss mechanistically cause invasive squamous cell cancers? Concordant p120ctn and E-cadherin loss is likely favoring cancer cell migration and invasion. Because

Figure 3. Histologic Analysis of Tumors from *L2Cre;p120ctn*$^{loxP/loxP}$ Mice

(A) H&E analyses of the esophagi, forestomachs, and oral cavities of 12-month-old *L2Cre;p120ctn*$^{loxP/loxP}$ mice (n = 17) revealed invasive squamous cell cancers. All control mice (five p120ctn$^{loxP/loxP}$, ten *L2Cre;p120ctn*$^{+/+}$, and eight *L2Cre;p120ctn*$^{+/loxP}$) had no lesions. The bottom row of images denotes higher magnification views of *L2Cre;p120ctn*$^{loxP/loxP}$ mice containing regions of invasive cancer (denoted by arrows). WD, well-differentiated tumor; PD, poorly differentiated tumor. Scale bars, 50 μM.

(B) IHC staining of 12-month-old mice for E-cadherin expression (four for each genotype). Arrow indicates normal membrane localization. Asterisks indicate loss of E-cadherin expression, and arrowhead indicates cytoplasmic localization of residual E-cadherin expression. Scale bars, 50 μM.

(C) IF of the esophagi and oral cavities of *L2Cre;p120ctn*$^{+/+}$ and *L2Cre;p120ctn*$^{loxP/loxP}$ mice (four for each) for p120ctn (red)-E-cadherin (green) costaining, K14 staining, and β-catenin staining. Arrows denote occasional regions of p120ctn and E-cadherin colocalization. K14 expression was detected in invading cells of both cancer types. β-Catenin was retained but mislocalized to the cytoplasm in esophageal tumors. By contrast, β-catenin expression was lost in oral cavity tumors. Asterisks denote regions of invasive cancers. Scale bars, 50 μM. See also Figure S2.

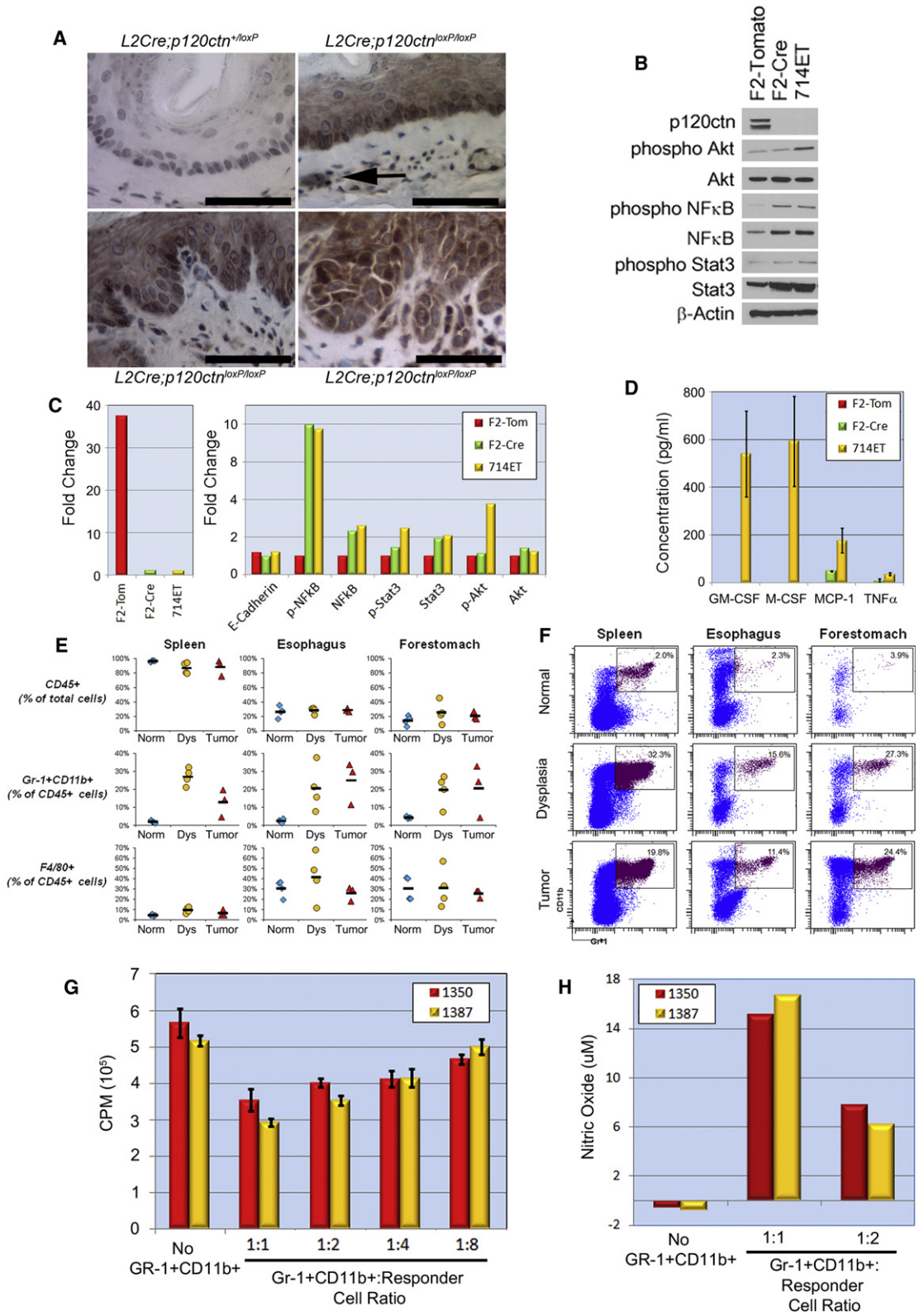

Figure 4. Immature Myeloid Cells Are Recruited to the Esophagi and Squamous Forestomachs of *L2Cre;p120ctn$^{loxP/loxP}$* Mice

(A) NFκB upregulation in *L2Cre;p120ctn$^{loxP/loxP}$ mice*. IHC staining for the NFκB p65 subunit revealed significant upregulation in hyperplastic, dysplastic, and invasive cancer lesions in the esophagi of *L2Cre;p120ctn$^{loxP/loxP}$* mice (n = 6). Arrows denote NFκB nuclear staining in immune cells within the stroma in *L2Cre;p120ctn$^{loxP/loxP}$* mice. Interestingly, these cells were found in early hyperplastic lesions. Scale bars, 50 μM.

p120ctn loss precedes E-cadherin loss in our model system, it is unclear to what extent there is a dependence upon E-cadherin loss.

E-cadherin destabilization or loss contributes to tumorigenesis. These squamous cancers induce prosurvival signals with NF-κB, Akt, and p-Stat3 activation. In contrast to p120ctn loss in skin with activated MAPK (Perez-Moreno et al., 2006), p120ctn loss in oral and esophageal keratinocytes does not have enhanced MAPK signaling. These squamous cell cancers have striking features of desmoplasia and immune cell infiltration, with significant increases in immature myeloid cells, but not in T cells, B cells, NK cells, dendritic cells, and macrophages. The precise recapitulation of human ESCC (along with OSCC) by the conditional deletion of p120ctn is remarkable, and a definitive in vivo genetic demonstration of p120ctn deletion resulting in cancer.

The Tumor Microenvironment Is Critical in Mediating the Effects of p120-ctn Loss

The tumor microenvironment is an array of diverse cell types that cooperate to foster tumor cell migration and invasion. The extracellular matrix includes invading tumor cells, fibroblasts (CAFs), endothelial cells, pericytes, and immune cells (Andreu et al., 2010; DeNardo et al., 2010; Kalluri and Zeisberg, 2006; Lewis and Pollard, 2006).

Immature myeloid cell recruitment has been noted by *IL-1β* overexpression in the stomach with resulting inflammation and cancer (Tu et al., 2008), disruption of TGFβ signaling in mammary carcinomas (Yang et al., 2008), knock in of mutant *K-ras* to the pancreas (Clark et al., 2007), and preparing the local pulmonary environment for metastasis (Yan et al., 2010). We observed a significant increase in immature myeloid cells in the tumor microenvironment and the spleen. It is conceivable that GM-CSF secreted by tumors contributes to the recruitment of immature myeloid cells (Marigo et al., 2010). We do not find evidence of increased IL-1β, IL-6, VEGF, and prostaglandins from the tumor cells, which have been linked also to the recruitment of immature myeloid cells (Ostrand-Rosenberg and Sinha, 2009). Other cell types in the tumor microenvironment might serve as the sources for these other cytokines.

How do immature myeloid cells contribute to tumorigenesis? Immature myeloid cells have the ability to suppress antigen-specific T cell responses in vitro (Gabrilovich et al., 2001; Gallina et al., 2006; Sinha et al., 2005). In our model system, immature myeloid cells isolated from tumor-bearing mice also have the ability to inhibit T cell activation. Additionally, the immature myeloid cells activate normal fibroblasts and augment activation of CAFs based upon Fsp1 and αSMA expression, which are novel findings. In turn, CAFs in our system contribute to prolonged survival of immature myeloid cells. We cannot exclude other protumorigenic functions of immature myeloid cells in our model system related to angiogenesis, secretion of chemokines/cytokines, and production of ECM-degrading enzymes (DeNardo et al., 2009, 2010; Ferrara, 2010; Gabrilovich and Nagaraj, 2009; Ostrand-Rosenberg and Sinha, 2009; Yang et al., 2004, 2008). Because dexamethasone has protean effects, it will be important to ablate immature myeloid cells in a specific fashion in our model system and in those models where immature myeloid cells are thought to be critical.

In summary, conditional p120ctn loss in the esophagus, oral cavity, and forestomach leads to invasive squamous cell cancers, involving NFκB, Akt, Stat-3 activation, increased proliferation, and production of GM-CSF, M-CSF, MCP-1, and TNFα from tumor-derived cells. The accompanying tumor microenvironment is replete with desmoplasia and immature myeloid cells. These events likely contribute to cancer arising from p120ctn-deficient cells (Figure 7), which provide compelling evidence that p120ctn is indeed a bona fide tumor suppressor gene. Because the *L2-Cre;p120*$^{loxP/loxP}$ mice phenocopy human OSCC and ESCC, they serve as a model for the translational development of diagnostic and therapeutic agents, goals that have been hindered by the absence of robust, genetically based models. Furthermore, our model might be applicable to other squamous cancers given common genomic alterations between ESCC and lung SCC where SOX-2 is amplified (Bass et al., 2009). Several approaches merit consideration in this context. First, strategies designed to restore wild-type p120ctn may provide a venue to ameliorate tumor progression. Given the complex nature of the tumor microenvironment, targeting of components, either individually or in combination, might advance the field. For example, prodrugs have been demonstrated to be efficacious against fibroblast activation protein (FAP) in prostate cancer (Lebeau et al., 2009). Strategies to target immature myeloid cells might be attractive based upon our studies as well in pancreatic cancer (Clark et al., 2007).

(B) Western blot analysis of mouse-derived cell lines (F2-Tomato, F2-Cre, 714ET; see Experimental Procedures) were used to investigate p120ctn loss as well as Akt, NFκB, and Stat3 activation (performed in triplicate). β-Actin is used as a loading control.
(C) Densitometry of western blot data from (B). All data are normalized to β-actin.
(D) Cytokine analysis of conditioned media from F2-Tomato, F2-Cre, and 714 ET cells (three for each cell line). ELISAs revealed increased GM-CSF ($p = 0.040$), M-CSF ($p = 0.035$), MCP-1 ($p = 0.026$), and TNFα ($p = 0.005$) in 714ET cells and increased MCP-1 in F2-Cre cells ($p = 1.6 \times 10^{-5}$). Nondetectable ELISA readings were given a value of zero for graphical purposes.
(E) Flow cytometry for CD45+ (total leukocytes) cells, Gr-1+ CD11b+ (immature myeloid) cells, and F4/80+ macrophages in the spleen (left), esophagus (middle), and forestomach (right) of control mice (*L2Cre;p120ctn*$^{+/+}$, blue diamonds; n = 4), *L2Cre;p120ctn*$^{loxP/loxP}$ mice with dysplasia (yellow circles; n = 4), and tumor-bearing (TB) *L2Cre;p120ctn*$^{loxP/loxP}$ mice (red triangles; n = 3). Black horizontal bars are mean percentages for each group. See p values in Figure S3.
(F) Representative flow cytometric results from (E) are depicted. Cells from the spleen (left), esophagus (middle), and forestomach (right) were gated for CD45 expression and then analyzed for Gr-1 (x axis) versus CD11b (y axis) expression. Numbers represent percentages of Gr-1+ CD11b+ (immature myeloid cells) among CD45+ cells.
(G) Proliferation assay for T cells cocultured with Gr-1+CD11b+ cells at the indicated cell ratios. Gr-1+CD11b+ cells suppressed T cell proliferation (n = 6). As the ratio of Gr-1+CD11b+ cells relative to T cells decreased, T cell proliferation increased (two with 1350, 1387 representing *L2Cre;p120ctn*$^{loxP/loxP}$ mice). All p values are <0.05 except 1:8 ratio for mouse 1387 when compared to no Gr-1+CD11b+ cells. (H) Nitric oxide (NO) in the conditioned media was determined (two *L2Cre;p120ctn*$^{loxP/loxP}$ mice, 1350, 1387). NO levels were increased in a titratable manner. Error bars indicate SEM. See also Table S2 and Figure S3.

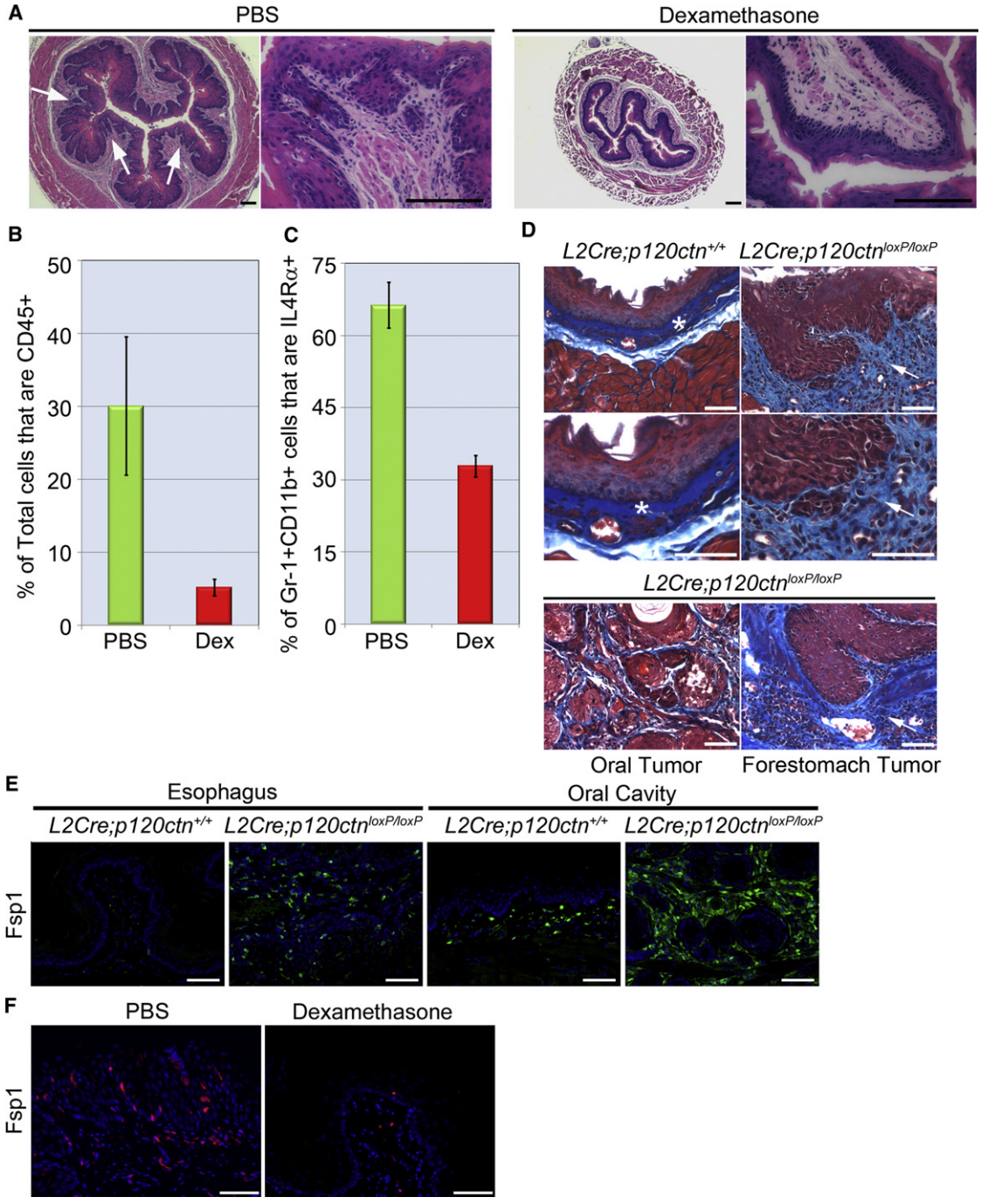

Figure 5. The Immune Response Is Involved in the Tumor Microenvironment in *L2Cre;p120ctn$^{loxP/loxP}$* Mice

(A) Dexamethasone (Dex) or PBS (control) was administered to 8-month-old *L2Cre;p120ctn$^{loxP/loxP}$* mice (five in each group) for 7 days. Histologic examination of the esophagi revealed hyperplasia without desmoplasia or inflammation in the Dex-treated mice, whereas invasive esophageal squamous cancer with desmoplasia and inflammation was present in PBS-treated mice. Arrows point to regions of invasion. Scale bars, 100 μM.

(B) FACS analysis for CD45+ cells contained within the esophagi from Dex-treated mice (red bars) and PBS control mice (green bars) (five in each group; p = 0.01). Dex treatment reduced CD45+ and Gr-1+CD11b+ cells by 6-fold.

(C) FACS analysis for IL-4Rα+ cells contained within the Gr-1+CD11b+ population of cells from Dex-treated mice (red bars) and PBS control mice (green bars) (five in each group; p = 0.0016). Dex reduced the percentage of Gr-1+ CD11b+ cells that express IL-4Rα by about 50%.

(D) Masson's trichrome staining on esophagi of *L2Cre;p120ctn$^{loxP/loxP}$* mice (n = 4) and control (*L2Cre;p120ctn$^{+/+}$*) mice. Asterisks indicate the fibrillar collagen layer in the control *L2Cre;p120ctn$^{+/+}$* esophagi. Arrows indicate the abundant fibrillar collagen surrounding invasive esophageal tumors (upper right and lower right panels). Invasive oral and forestomach tumors in *L2Cre;p120ctn$^{loxP/loxP}$* mice are depicted in the bottom row. Arrows indicate the staining surrounding invasive cancers. Scale bars, 50 μM.

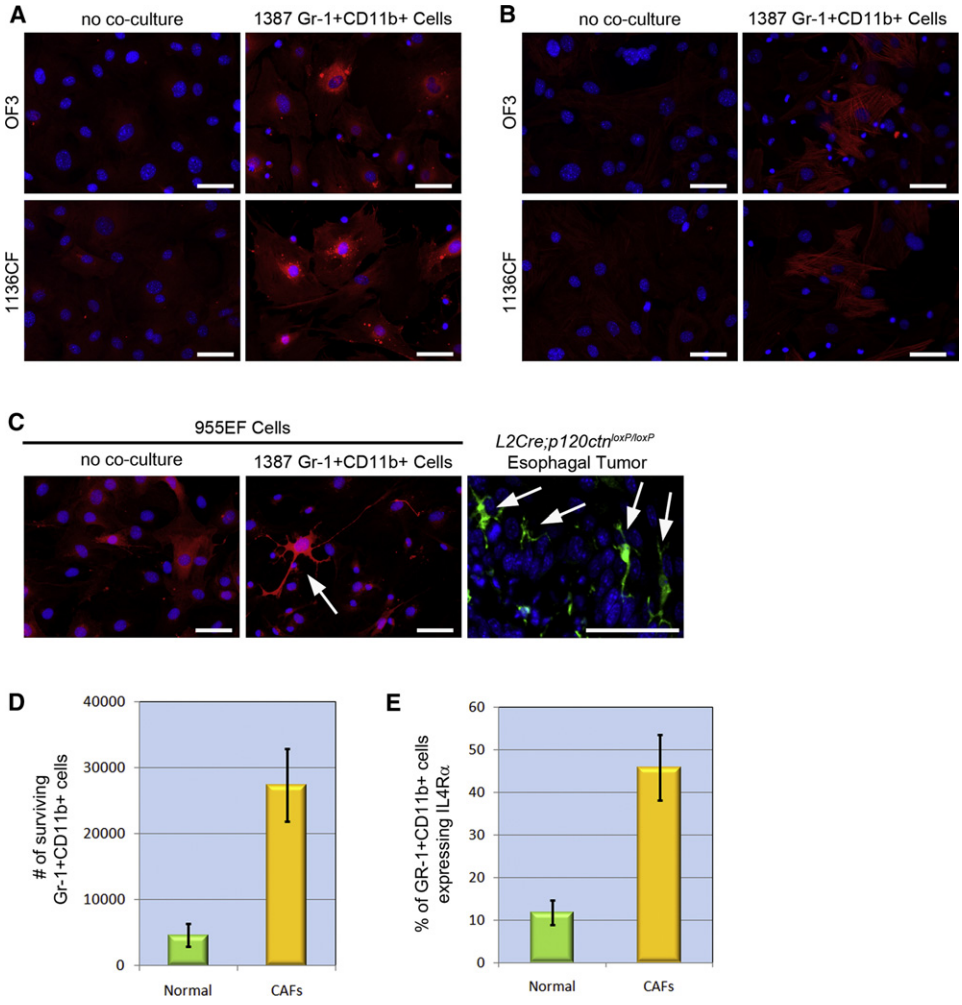

Figure 6. Crosstalk between Immature Myeloid Cells and Fibroblasts in the Tumor Microenvironment of *L2Cre;p120ctn$^{loxP/loxP}$* Mice

(A) Fibroblasts from the oral cavity of wild-type mice (designated as OF3) or oral CAFs [designated as 1136CF]) from *L2Cre;p120ctn$^{loxP/loxP}$* mice were analyzed in coculture with Gr-1+CD11b+ cells for Fsp1 expression by IF. Cocultured fibroblasts had increased Fsp1 expression (n = 6). Scale bars, 50 μM.

(B) Cocultured fibroblasts had increased αSMA expression (n = 6). Scale bars, 50 μM.

(C) An esophageal CAF cell line (955EF) had high basal Fsp1 expression when cultured alone. Coculturing of 955EF cells (n = 6) resulted in even higher Fsp1 expression. Note that the highest Fsp1+ 955EF cells have "dendrite-like" projections, which is evident also in esophageal tumors from *L2Cre;p120ctn$^{loxP/loxP}$* mice (n = 4). Scale bars, 50 μM.

(D) FACS revealed increased survival of Gr-1+CD11b+ cells in coculture with CAFs (n = 4; p = 0.021). (E) FACS demonstrated increased IL-4Rα expression in Gr-1+CD11b+ cells in coculture with CAFs (n = 4; p = 0.016). Error bars indicate SEM.

EXPERIMENTAL PROCEDURES

Cell Lines

TE and HCE cells, all established human esophageal squamous cancer cell lines, were cultivated in DMEM media supplemented by 10% fetal calf serum (Sigma-Aldrich) and 1% penicillin/streptomycin (Invitrogen) and grown in 5% CO_2 conditions as described previously (Okano et al., 2000). Cell lines were established from mouse esophageal tumors (designated as 714ET), mouse fibroblasts (designated as OF3 from normal oral cavity), and mouse CAFs (designated as 1136CF from OSCC and designated as 955EF from ESCC) and verified to be of epithelial or fibroblast origin. The mouse cell lines were cultivated in DMEM as above.

To generate pBABE-tdTomato-SV40-nlsCre (6982 bp), puromycin acetyltransferase of pBABE-puro was replaced with nlsCre cDNA derived from pHRnlsCre (Addgene), and then tdTomato cDNA (gift of Roger Y. Tisen, University of California, San Diego, San Diego, CA, USA) was subcloned. The parental F2 cells were established through the isolation of esophageal epithelia (Opitz et al., 2002) from *p120$^{loxP/loxP}$* mice, infected with pBABE-tdTomato-SV40-nlsCre (designated as F2-Cre) or pBABE-tdTomato (designated as F2-Tomato), and stable clones were FACS selected for tdTomato. The

(E) Fsp1 IF with increased expression in esophageal and oral cavity tumors from *L2Cre;p120ctn$^{loxP/loxP}$* mice (n = 4) compared to control *L2Cre;p120ctn$^{+/+}$* mice (n = 4) tissues. Scale bar, 50 μM.

(F) Fsp1 IF of esophagi from *L2Cre;p120ctn$^{loxP/loxP}$* mice treated with either PBS or Dex from Figure 5A. Fsp1 expression is decreased in Dex-treated mice (n = 5) when compared to PBS treated mice (n = 5). Scale bars, 50 μM. See also Figure S4. Error bars indicate SEM.

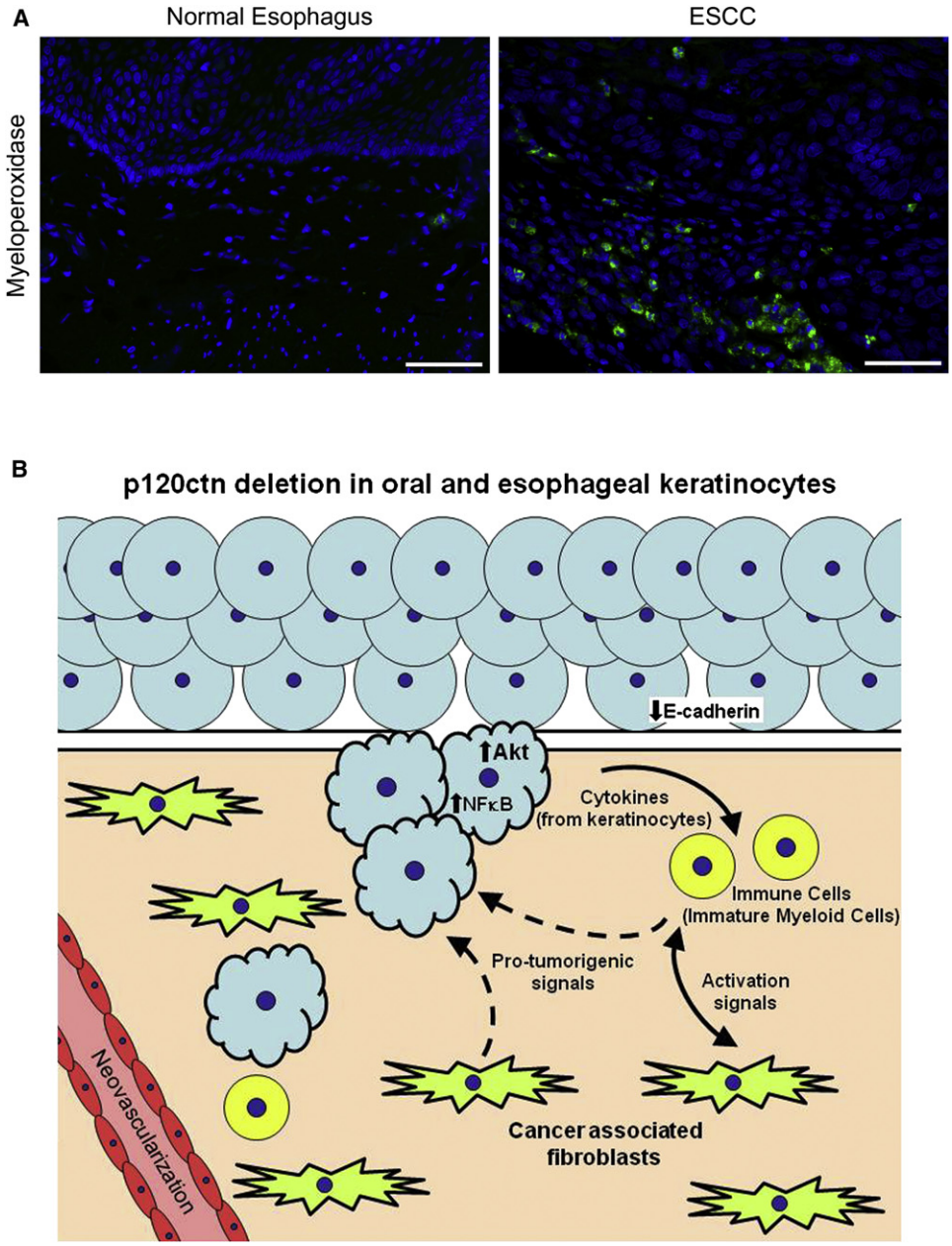

Figure 7. MPO Expression in Human ESCC

(A) MPO expression was analyzed by IF in 14 ESCC samples with matched adjacent normal esophageal mucosa. Representative image is depicted with MPO-positive cells present in the tumor stroma (right panel). MPO staining was increased in the tumor stroma and correlates with p120ctn loss ($p = 0.05$, Fisher's exact analysis). Scale bars, 50 μM.

(B) Model of OSCC and ESCC in conditional p120ctn-deleted mice. Solid lines represent cell-cell interactions emerging from experiments in this study. Dashed lines are potential areas of interactions. See also Figure S5.

F2-Cre and F2-Tomato cell lines were cultivated in KSFM as described previously (Andl et al., 2003; Harada et al., 2003).

Histology and IHC/IF

Paraffin tissue sectioning and staining for hematoxylin and eosin (H&E) and IHC were performed as described previously (Stairs et al., 2008). Antibodies used for IHC were the following: p120ctn (610134; BD Transduction); E-cadherin (610182; BD Transduction); K14 (PRB-155P; Covance); pAKT (9271; Cell Signaling); pMAPK (9101; Cell Signaling); NFκB-p65 subunit (4764; Cell Signaling); and Ki67 (NCL-KI67p; Novacastra). For IF the following antibodies were used: K14 (PRB-155P; Covance); Fsp1 (DakoCytomation); β-catenin (9562; Cell Signaling); p120ctn (61634; BD Transduction); E-cadherin (3195; Cell Signaling); c-*myc* (1472-1; Epitomics); MPO (45977; Abcam); p-Stat3 (9145; Cell Signaling); and αSMA (A2547; Sigma). Secondary antibodies used were: Alexa Fluor 488-anti-rabbit, Alexa Fluor 568 anti-rat, or Alexa Fluor 568 anti-mouse. Slides were coverslipped using VectaShield mounting medium with DAPI.

TMAs

TMAs were created using 69 matched paraffin blocks from de-identified patients with primary ESCC and adjacent normal esophageal tissues (with Institutional Review Board exempt status for the TMA due to the de-identification). Scoring of p120ctn, E-cadherin, and MPO IHC was based upon a quantitative evaluation of expression using a scale from 0 to 2 (0, absent; 1, mild-moderate; 2, high) and performed by A.K.-S., pathologist, in a blinded fashion. Fisher's exact test was used.

Generation of Mouse Models

The Institutional Animal Care and Use Committee (IACUC) at the University of Pennsylvania approved all animal studies. Mice were housed under a 12-hr light/dark cycle and fed ad libitum. *LoxP*-flanked *p120ctn* mice were generated previously (Davis and Reynolds, 2006). *L2Cre* transgenic mice were generated by cloning Cre recombinase under the control of the EBV ED-L2 promoter (Nakagawa et al., 1997; Opitz et al., 2002). Mice were genotyped for the *LoxP* allele as described previously (Davis and Reynolds, 2006). Mice were genotyped for *L2Cre* by PCR analysis using primers contained within the Cre (forward: GGCCAGCTAAACATGCTTCATCGT; reverse: ACGTAACAGGGTGTTATAAGCAAT). PCR conditions were 35 cycles at 94°C for 45 s, 61°C for 45 s, and 72°C for 1 min, 30 s. Additionally, *L2Cre* mice were bred with *Gt(Rosa)*^{26Tm1Sor} reporter mice, and tissues were subjected to LacZ staining as described previously (Brembeck et al., 2001).

Dexamethasone Treatment

L2-Cre;p120$^{loxP/loxP}$ mice were injected intraperitoneally with either dexamethasone 10 mg/kg/day or PBS (control) for 7 days. After 7 days, mice were sacrificed, and the esophagi and spleens were excised for histology and FACS analysis.

Flow Cytometry

Single-cell suspensions of fresh spleens, esophagi, and squamous forestomachs were prepared from genetically engineered mice and littermate controls. Spleens were crushed and passed through a 70 μm cell strainer, treated with ACK Lysis Buffer (Invitrogen) and washed twice with RPMI/10% FCS. Esophagi and forestomachs were minced into 1–2 mm pieces, incubated in 1 mg/ml collagenase (Sigma-Aldrich) in RPMI for 45 min at 37°C, and then were passed through a 70 μm cell strainer and washed once with RPMI/10% FCS. Cells were stained in PBS/0.5% FCS with the following antibodies: CD45 (clone 30-F11), CD11c (clone HL3), Gr-1 (clone RBG-8C5), CD11b (clone M1/70), CD3ε (clone 145-2C11), CD49b (clone DX5), CD19 (clone 1D3), CD124 (clone mIL-4R-M1), and rat IgG2a, κ (clone R35-95) from BD Biosciences PharMingen and F4/80 (clone C1:A3-1) from AbD Serotec. Flow cytometry was done using a BD FACSCanto (BD Biosciences Immunocytometry Systems), and data were analyzed with BD FACSDiva software.

Gr-1+ CD11b+ Cell Isolation and Functional T Cell Suppression Assay

Gr-1+ CD11b+ cells were isolated from spleens using biotinylated anti-Gr-1 mAb, magnetic beads, and MiniMACS columns (Miltenyi Biotec). The purity was >90% Gr-1+ CD11b+ cells by flow cytometry. Antigen-specific suppression of CD8+ T cells was evaluated using splenocytes from OT-1 transgenic mice as responder cells. OT-1 splenocytes were seeded in triplicates in 96-well round-bottom plates (7×10^5/well) and stimulated with cognate antigen, OVA-derived peptide SIINFEKL (1 μg/ml; New England Peptide), and cultured for 4 days in the presence of increasing ratios of Gr-1+ CD11b+ cells. Eighteen hours before harvesting, cells were pulsed with [^{3}H]thymidine (1 μCi per well; Amersham Biosciences). [^{3}H]Thymidine incorporation was assessed using a liquid scintillation counter and expressed as cpm. Student's t test was used.

NO Production

NO production by Gr-1+ CD11b+ cells was evaluated in culture supernatant from T cell suppression assays using the Griess Reagent System (Promega). Equal volumes of culture supernatant (40 μl) were mixed with 1% sulfanilamide in 5% phosphoric acid and incubated at RT for 10 min, followed by addition of 0.1% N-1-naphthylethylenediamine dihydrochloride in water. After a 10-min incubation at RT, absorbance (550 nm) was measured using a microplate reader. Nitrite concentrations were determined by comparing the absorbance for the test samples to a standard curve generated by serial dilution of 0.1 mM sodium nitrite. Student's t test was used.

Coculture of Immature Myeloid Cells and Fibroblasts

Immature myeloid cells were cocultured with fibroblasts for 96 hr, and fibroblasts were evaluated for αSMA and Fsp1. Immature myeloid cells were evaluated for survival and IL-Rα expression. Student's t test was used.

Cytology of Gr-1+ CD11b+ Cells

Gr-1+ CD11b+ cells were purified (>98%) from spleens of tumor-bearing mice using a MoFlo fluorescence activated cell sorter (DakoCytomation). Cytospin preparations were stained with Diff-Quick reagent and by IF for NFκB.

Cytokine Analysis

The following cytokines were measured either by BD Cytokine Bead Array (BD Biosciences) or by ELISA (R&D Systems): IL-1β, IL-2, IL-4, IL-5, IL-6, IFNγ, TNFα, GM-CSF, G-CSF, MCP-1, KC, M-CSF, SCF, and VEGF.

RNA Microarrays

The epithelia from mouse esophagi and squamous forestomachs were isolated by digesting the tissues with a 1:2 dilution dispase (BD) in deionized water at 37°C for 5–10 min. The epithelia were peeled and snap-frozen and stored at −80°C for RNA isolation. RNA was purified, and cRNA was prepped (Affymetrix) and run on Affymetrix Mouse 1.0ST Affymetrix Arrays.

Statistical Analysis of RNA Microarray Data

Gene expression differences were considered statistically significant if the p value was less than 0.01. A global test was done as to whether the expression profiles differed between the classes by permuting the labels of which arrays corresponded to which classes. For each permutation the p values were recomputed, and the number of genes significant at the 0.01 level was noted. The false discovery rate was estimated to be less than 10%. Cluster analysis was performed with Cluster and TreeView software (Eisen et al., 1998).

ACCESSION NUMBERS

Coordinates have been deposited in the GEO database with accession code GSE20240.

SUPPLEMENTAL INFORMATION

Supplemental Information includes five figures, two tables, and Supplemental Experimental Procedures, and can be found with this article online at doi:10.1016/j.ccr.2011.02.007.

ACKNOWLEDGMENTS

This work was supported by the following NIH grants: NCI P01-CA098101 Mechanisms in Esophageal Carcinogenesis (to D.B.S., J.K., M.E.V., J.P.K., A.K.-S., J.A.D., and A.K.R.); NCI F32-CA1308513 and NCI K99/R00-CA138498 (to D.B.S.); NCI T32-CA115299 (to J.K.); NCI U01-CA143056 (to A.K.R.); NCI P30 Abramson Cancer Center pilot grant NCI P30-CA016520 (to R.H.V.); NIDDK R01-DK069984 (to J.P.K.); and the NIDDK P30-DK050306 Center for Molecular Studies in Digestive and Liver Diseases and the American Cancer Society Research Professorship (to A.K.R.). Work contributed by the Reynolds lab was supported by NCI CA111947, CA055724, and the Vanderbilt GI SPORE (50CA95103). We wish to thank the Morphology (S. Mitchell), Molecular Biology/Gene Expression, Transgenic/Chimeric Mouse, Microarray and Cell Culture Core Facilities as well as Amy Ziober in the Department of Pathology and Laboratory Medicine. We are also grateful to members of the Rustgi lab for helpful discussions.

Received: January 22, 2010
Revised: October 5, 2010
Accepted: February 4, 2011
Published: April 11, 2011

REFERENCES

Anastasiadis, P.Z., Moon, S.Y., Thoreson, M.A., Mariner, D.J., Crawford, H.C., Zheng, Y., and Reynolds, A.B. (2000). Inhibition of RhoA by p120 catenin. Nat. Cell Biol. *2*, 637–644.

Andl, C.D., Mizushima, T., Nakagawa, H., Oyama, K., Harada, H., Chruma, K., Herlyn, M., and Rustgi, A.K. (2003). Epidermal growth factor receptor mediates increased cell proliferation, migration, and aggregation in esophageal keratinocytes in vitro and in vivo. J. Biol. Chem. *278*, 1824–1830.

Andreu, P., Johansson, M., Affara, N.I., Pucci, F., Tan, T., Junankar, S., Korets, L., Lam, J., Tawfik, D., DeNardo, D.G., et al. (2010). FcRgamma activation regulates inflammation-associated squamous carcinogenesis. Cancer Cell *17*, 121–134.

Bartlett, J.D., Dobeck, J.M., Tye, C.E., Perez-Moreno, M., Stokes, N., Reynolds, A.B., Fuchs, E., and Skobe, Z. (2010). Targeted p120-catenin ablation disrupts dental enamel development. PLoS ONE *5*, e12703.

Bass, A.J., Watanabe, H., Mermel, C.H., Yu, S., Perner, S., Verhaak, R.G., Kim, S.Y., Wardwell, L., Tamayo, P., Gat-Viks, I., et al. (2009). SOX2 is an amplified lineage-survival oncogene in lung and esophageal squamous cell carcinomas. Nat. Genet. *41*, 1238–1242.

Birchmeier, W. (1995). E-cadherin as a tumor (invasion) suppressor gene. Bioessays *17*, 97–99.

Brembeck, F.H., Moffett, J., Wang, T.C., and Rustgi, A.K. (2001). The keratin 19 promoter is potent for cell-specific targeting of genes in transgenic mice. Gastroenterology *120*, 1720–1728.

Bronte, V., and Zanovello, P. (2005). Regulation of immune responses by L-arginine metabolism. Nat. Rev. Immunol. *5*, 641–654.

Bronte, V., Serafini, P., Mazzoni, A., Segal, D.M., and Zanovello, P. (2003). L-arginine metabolism in myeloid cells controls T-lymphocyte functions. Trends Immunol. *24*, 302–306.

Chung, Y., Lam, A.K., Luk, J.M., Law, S., Chan, K.W., Lee, P.Y., and Wong, J. (2007). Altered E-cadherin expression and p120 catenin localization in esophageal squamous cell carcinoma. Ann. Surg. Oncol. *14*, 3260–3267.

Clark, C.E., Hingorani, S.R., Mick, R., Combs, C., Tuveson, D.A., and Vonderheide, R.H. (2007). Dynamics of the immune reaction to pancreatic cancer from inception to invasion. Cancer Res. *67*, 9518–9527.

Davis, M.A., and Reynolds, A.B. (2006). Blocked acinar development, E-cadherin reduction, and intraepithelial neoplasia upon ablation of p120-catenin in the mouse salivary gland. Dev. Cell *10*, 21–31.

Davis, M.A., Ireton, R.C., and Reynolds, A.B. (2003). A core function for p120-catenin in cadherin turnover. J. Cell Biol. *163*, 525–534.

DeNardo, D.G., Barreto, J.B., Andreu, P., Vasquez, L., Tawfik, D., Kolhatkar, N., and Coussens, L.M. (2009). CD4(+) T cells regulate pulmonary metastasis of mammary carcinomas by enhancing protumor properties of macrophages. Cancer Cell *16*, 91–102.

DeNardo, D.G., Andreu, P., and Coussens, L.M. (2010). Interactions between lymphocytes and myeloid cells regulate pro- versus anti-tumor immunity. Cancer Metastasis Rev. *29*, 309–316.

Eisen, M.B., Spellman, P.T., Brown, P.O., and Botstein, D. (1998). Cluster analysis and display of genome-wide expression patterns. Proc. Natl. Acad. Sci. USA *95*, 14863–14868.

Ferrara, N. (2010). Role of myeloid cells in vascular endothelial growth factor-independent tumor angiogenesis. Curr. Opin. Hematol. *17*, 219–224.

Fukumoto, Y., Shintani, Y., Reynolds, A.B., Johnson, K.R., and Wheelock, M.J. (2008). The regulatory or phosphorylation domain of p120 catenin controls E-cadherin dynamics at the plasma membrane. Exp. Cell Res. *314*, 52–67.

Gabrilovich, D.I., and Nagaraj, S. (2009). Myeloid-derived suppressor cells as regulators of the immune system. Nat. Rev. Immunol. *9*, 162–174.

Gabrilovich, D.I., Velders, M.P., Sotomayor, E.M., and Kast, W.M. (2001). Mechanism of immune dysfunction in cancer mediated by immature Gr-1+ myeloid cells. J. Immunol. *166*, 5398–5406.

Gallina, G., Dolcetti, L., Serafini, P., De Santo, C., Marigo, I., Colombo, M.P., Basso, G., Brombacher, F., Borrello, I., Zanovello, P., et al. (2006). Tumors induce a subset of inflammatory monocytes with immunosuppressive activity on CD8+ T cells. J. Clin. Invest. *116*, 2777–2790.

Harada, H., Nakagawa, H., Oyama, K., Takaoka, M., Andl, C.D., Jacobmeier, B., von Werder, A., Enders, G.H., Opitz, O.G., and Rustgi, A.K. (2003). Telomerase induces immortalization of human esophageal keratinocytes without p16INK4a inactivation. Mol. Cancer Res. *1*, 729–738.

Ireton, R.C., Davis, M.A., van Hengel, J., Mariner, D.J., Barnes, K., Thoreson, M.A., Anastasiadis, P.Z., Matrisian, L., Bundy, L.M., Sealy, L., et al. (2002). A novel role for p120 catenin in E-cadherin function. J. Cell Biol. *159*, 465–476.

Ishiyama, N., Lee, S.H., Liu, S., Li, G.Y., Smith, M.J., Reichardt, L.F., and Ikura, M. (2010). Dynamic and static interactions between p120 catenin and E-cadherin regulate the stability of cell-cell adhesion. Cell *141*, 117–128.

Kalluri, R., and Zeisberg, M. (2006). Fibroblasts in cancer. Nat. Rev. Cancer *6*, 392–401.

Lebeau, A.M., Brennen, W.N., Aggarwal, S., and Denmeade, S.R. (2009). Targeting the cancer stroma with a fibroblast activation protein-activated promelittin protoxin. Mol. Cancer Ther. *8*, 1378–1386.

Lewis, C.E., and Pollard, J.W. (2006). Distinct role of macrophages in different tumor microenvironments. Cancer Res. *66*, 605–612.

Macpherson, I.R., Hooper, S., Serrels, A., McGarry, L., Ozanne, B.W., Harrington, K., Frame, M.C., Sahai, E., and Brunton, V.G. (2007). p120-catenin is required for the collective invasion of squamous cell carcinoma cells via a phosphorylation-independent mechanism. Oncogene *26*, 5214–5228.

Mandruzzato, S., Solito, S., Falisi, E., Francescato, S., Chiarion-Sileni, V., Mocellin, S., Zanon, A., Rossi, C.R., Nitti, D., Bronte, V., and Zanovello, P. (2009). IL4Ralpha+ myeloid-derived suppressor cell expansion in cancer patients. J. Immunol. *182*, 6562–6568.

Marigo, I., Bosio, E., Solito, S., Mesa, C., Fernandez, A., Dolcetti, L., Ugel, S., Sonda, N., Bicciato, S., Falisi, E., et al. (2010). Tumor-induced tolerance and immune suppression depend on the C/EBPbeta transcription factor. Immunity *32*, 790–802.

Nakagawa, H., Wang, T.C., Zukerberg, L., Odze, R., Togawa, K., May, G.H., Wilson, J., and Rustgi, A.K. (1997). The targeting of the cyclin D1 oncogene by an Epstein-Barr virus promoter in transgenic mice causes dysplasia in the tongue, esophagus and forestomach. Oncogene *14*, 1185–1190.

Okano, J., Gaslightwala, I., Birnbaum, M.J., Rustgi, A.K., and Nakagawa, H. (2000). Akt/protein kinase B isoforms are differentially regulated by epidermal growth factor stimulation. J. Biol. Chem. *275*, 30934–30942.

Opitz, O.G., Harada, H., Suliman, Y., Rhoades, B., Sharpless, N.E., Kent, R., Kopelovich, L., Nakagawa, H., and Rustgi, A.K. (2002). A mouse model of human oral-esophageal cancer. J. Clin. Invest. *110*, 761–769.

Ostrand-Rosenberg, S., and Sinha, P. (2009). Myeloid-derived suppressor cells: linking inflammation and cancer. J. Immunol. *182*, 4499–4506.

Perez-Moreno, M., Davis, M.A., Wong, E., Pasolli, H.A., Reynolds, A.B., and Fuchs, E. (2006). p120-catenin mediates inflammatory responses in the skin. Cell *124*, 631–644.

Perez-Moreno, M., Song, W., Pasolli, H.A., Williams, S.E., and Fuchs, E. (2008). Loss of p120 catenin and links to mitotic alterations, inflammation, and skin cancer. Proc. Natl. Acad. Sci. USA *105*, 15399–15404.

Reynolds, A.B., and Roczniak-Ferguson, A. (2004). Emerging roles for p120-catenin in cell adhesion and cancer. Oncogene *23*, 7947–7956.

Schreck, R., and Baeuerle, P.A. (1990). NF-kappa B as inducible transcriptional activator of the granulocyte-macrophage colony-stimulating factor gene. Mol. Cell. Biol. *10*, 1281–1286.

Sinha, P., Clements, V.K., and Ostrand-Rosenberg, S. (2005). Reduction of myeloid-derived suppressor cells and induction of M1 macrophages facilitate the rejection of established metastatic disease. J. Immunol. *174*, 636–645.

Smalley-Freed, W.G., Efimov, A., Burnett, P.E., Short, S.P., Davis, M.A., Gumucio, D.L., Washington, M.K., Coffey, R.J., and Reynolds, A.B. (2010). p120-catenin is essential for maintenance of barrier function and intestinal homeostasis in mice. J. Clin. Invest. *120*, 1824–1835.

Stairs, D.B., Nakagawa, H., Klein-Szanto, A., Mitchell, S.D., Silberg, D.G., Tobias, J.W., Lynch, J.P., and Rustgi, A.K. (2008). Cdx1 and c-Myc foster

the initiation of transdifferentiation of the normal esophageal squamous epithelium toward Barrett's esophagus. PLoS ONE *3*, e3534.

Thoreson, M.A., and Reynolds, A.B. (2002). Altered expression of the catenin p120 in human cancer: implications for tumor progression. Differentiation *70*, 583–589.

Tu, S., Bhagat, G., Cui, G., Takaishi, S., Kurt-Jones, E.A., Rickman, B., Betz, K.S., Penz-Oesterreicher, M., Bjorkdahl, O., Fox, J.G., and Wang, T.C. (2008). Overexpression of interleukin-1beta induces gastric inflammation and cancer and mobilizes myeloid-derived suppressor cells in mice. Cancer Cell *14*, 408–419.

van Hengel, J., and van Roy, F. (2007). Diverse functions of p120ctn in tumors. Biochim. Biophys. Acta *1773*, 78–88.

Wildenberg, G.A., Dohn, M.R., Carnahan, R.H., Davis, M.A., Lobdell, N.A., Settleman, J., and Reynolds, A.B. (2006). p120-catenin and p190RhoGAP regulate cell-cell adhesion by coordinating antagonism between Rac and Rho. Cell *127*, 1027–1039.

Xiao, K., Allison, D.F., Buckley, K.M., Kottke, M.D., Vincent, P.A., Faundez, V., and Kowalczyk, A.P. (2003). Cellular levels of p120 catenin function as a set point for cadherin expression levels in microvascular endothelial cells. J. Cell Biol. *163*, 535–545.

Yan, H.H., Pickup, M., Pang, Y., Gorska, A.E., Li, Z., Chytil, A., Geng, Y., Gray, J.W., Moses, H.L., and Yang, L. (2010). Gr-1+CD11b+ myeloid cells tip the balance of immune protection to tumor promotion in the premetastatic lung. Cancer Res. *70*, 6139–6149.

Yang, L., DeBusk, L.M., Fukuda, K., Fingleton, B., Green-Jarvis, B., Shyr, Y., Matrisian, L.M., Carbone, D.P., and Lin, P.C. (2004). Expansion of myeloid immune suppressor Gr+CD11b+ cells in tumor-bearing host directly promotes tumor angiogenesis. Cancer Cell *6*, 409–421.

Yang, L., Huang, J., Ren, X., Gorska, A.E., Chytil, A., Aakre, M., Carbone, D.P., Matrisian, L.M., Richmond, A., Lin, P.C., and Moses, H.L. (2008). Abrogation of TGF beta signaling in mammary carcinomas recruits Gr-1+CD11b+ myeloid cells that promote metastasis. Cancer Cell *13*, 23–35.